Petroleum Science 21 (2024) 2806–2816

Contents lists available at ScienceDirect

Petroleum Science

journal homepage: www.keaipublishing.com/en/journals/petroleum-science

Original Paper

Construction of coal pitch-based HA-K grafted poly condensates and their excellent anti-temperature and viscosity-reducing properties

Jing Tan [a, b], Wei Zhang [c], Xiu-Ling Yan [a, **], Hao Zhou [b], Sher Bahadar Khan [e], Seitkhan Azat [f], Shi-You Yan [d], Hao-Jie Ma [d], Xin-Tai Su [a, b, *]

[a] Xinjiang Key Laboratory of Clean Conversion and High Value Utilization of Biomass Resources, College of Chemistry and Chemical Engineering, Yili Normal University, Yining, 835000, Xinjiang, China
[b] School of Environment and Energy, Guangdong Provincial Key Laboratory of Solid Wastes Pollution Control and Recycling, South China University of Technology, Guangzhou, 510006, Guangdong, China
[c] Drilling Fluid Branch of CNPC Xibu Drilling Engineering Company Limited, Karamay, 830046, Xinjiang, China
[d] Urumchi Huatailong Chemical Additives Co., Ltd., Urumqi, 830000, Xinjiang, China
[e] Department of Chemistry, Faculty of Science, King Abdulaziz University, PO Box 80203, Jeddah, 21589, Saudi Arabia
[f] Faculty of Chemistry and Chemical Technology, Al-Farabi Kazakh National University, Almaty, 050013, Kazakhstan

ARTICLE INFO

Article history:
Received 11 October 2023
Received in revised form
16 April 2024
Accepted 17 April 2024
Available online 18 April 2024

Edited by Min Li

Keywords:
Viscosity breaker
Heat resistance
Base mud
Graft CP-HA-K polymer
CP
Salt resistance

ABSTRACT

Humic acids (HAs) are widely used as filtrate and viscosity reducers in drilling fluids. However, their practical utility is limited due to poor stability in salt resistance and high-temperature resistance. High-temperature coal pitch (CP) is a by-product from coal pyrolysis above 650 °C. The substance's molecular structure is characterized by a dense arrangement of aromatic hydrocarbon and alkyl substituents. This unique structure gives it unique chemical properties and excellent drilling performance, surpassing traditional humic acids in drilling operations. Potassium humate is prepared from CP (CP-HA-K) by thermal catalysis. A new type of high-quality humic acid temperature-resistant viscosity-reducer (Graft CP-HA-K polymer) is synthesized with CP-HA-K, hydrolyzed polyacrylonitrile sodium salt (Na-HPAN), urea, formaldehyde, phenol and acrylamide (AAM) as raw materials. The experimental results demonstrate that the most favorable conditions for the catalytic preparation of CP-HA-K are 1 wt% catalyst dosage, 30 wt% KOH dosage, a reaction temperature of 250 °C, and a reaction time of 2 h, resulting in a maximum yield of CP-HA-K of 39.58%. The temperature resistance of the Graft CP-HA-K polymer is measured to be 177.39 °C, which is 55.39 °C higher than that of commercial HA-K. This is due to the abundant presence of amide, hydroxyl, and amine functional groups in the Graft CP-HA-K polymer, which increase the length of the carbon chains, enhance the electrostatic repulsion on the surface of solid particles. After being aged to 120 °C for a specified duration, the Graft CP-HA-K polymer demonstrates significantly higher viscosity reduction (42.12%) compared to commercial HA-K (C-HA-K). Furthermore, the Graft CP-HA-K polymer can tolerate a high salt concentration of 8000 mg·L^{-1}, measured after the addition of optimum amount of 3 wt% Graft CP-HA-K polymer. The action mechanism of Graft CP-HA-K polymer on high-temperature drilling fluid is that the Graft CP-HA-K polymer can increase the repulsive force between solid particles and disrupt bentonite's reticulation structure. Overall, this research provides novelty insights into the synthesis of artificial humic acid materials and the development of temperature-resistant viscosity reducers, offering a new avenue for the utilization of CP resources.

1. Introduction

Drilling fluid is the blood of drilling. The rheological properties of drilling fluid are significant for transporting cuttings, keeping borehole stability, and ensuring drilling safety (Camp et al., 2018; Lei et al., 2021). However, the viscosity and cutting force of drilling

* Corresponding author. Xinjiang Key Laboratory of Clean Conversion and High Value Utilization of Biomass Resources, College of Chemistry and Chemical Engineering, Yili Normal University, Yining, 835000, Xinjiang, China.
** Corresponding author.
E-mail address: suxintai827@163.com (X.-T. Su).

https://doi.org/10.1016/j.petsci.2024.04.009

fluid are often increased due to temperature rise, salt invasion, or agent failure (Becattini et al., 2017; Kelessidis et al., 2007; Luo et al., 2017; Mao et al., 2015, 2020; Sepehri et al., 2018; Wang et al., 2021). High density and high shear pressure can cause difficulties in pump start-up and cuttings extraction (Bennett and Larter, 2000; Da Câmara et al., 2021; Fuentes-Audén et al., 2008). Therefore, in the process of using and maintaining drilling fluid, it is often necessary to add different types of drilling aid to reduce the viscosity and shear force of drilling fluid to make it have appropriate rheological properties (Ghosh et al., 2020; Szczerski et al., 2013).

Drilling fluid additives are typically classified into three categories: mineral products, natural products and their derivatives, and general and specialty chemicals. The category of natural products and their derivatives includes lignin-based, cellulose-based, and humic acid-based additives. Additives belonging to the lignin and cellulose categories are prone to causing thickening of the drilling fluid and are also susceptible to microbial attack, thus severely limiting their application. Chang et al. (2019) synthesized a novel amphiphilic polymer filtrate reducer for water-based drilling fluids through layer-by-layer self-assembly of nano lignin. The results demonstrated that the synthesized nano lignin effectively reduced the filtrate loss of water-based drilling fluids, but it also significantly induced the thickening of the drilling fluid, posing challenges in shale cuttings extraction. Compared with them, humic acid is a potential agent for reducing viscosity in drilling fluids due to possessing various active functional groups, hydrophilicity, cation exchange capacity, adsorption, and dispersion capacity (Aguiar et al., 2013; Doskočil et al., 2018; Doulia et al., 2009; De Melo et al., 2016; Patrakov et al., 2010; Proidakov, 2009). However, traditional humic acid is mainly obtained from the animal and plant remains in weathered coal, lignite, and peat. Humic acids typically contain numerous reactive functional groups, including carboxyl and hydroxyl groups, which can be susceptible to thermal decomposition or oxidation reactions under high-temperature conditions. As a result, their use in high-temperature environments is limited. and the temperature resistance is generally within 100 °C. Furthermore, humic acid tends to exhibit poor stability in high-salinity environments, and its salt resistance is typically 1000 mg·L^{-1}. High concentrations of salt solutions can cause reactions between humic acids and salt ions, resulting in precipitation or coagulation. This reduces their solubility and activity. Additionally, traditional humic acids have limited solubility in water and tend to form colloidal substances. In high-temperature environments, these colloidal substances are prone to aggregation and sedimentation, which increases viscosity (De Melo et al., 2016). The use of traditional humic acids may be restricted in high-salinity water bodies or high-temperature drilling environments. For instance, Apostolidou et al. (2022) studied the effectiveness of low-grade lignite as a shear thinning additive for influencing the rheological behavior and filtration control of drilling fluids that undergo dynamic thermal aging. The study found that lignite, when used as a shear-thinning additive, exhibited a yield point that tended towards or reached 0 mPa·s after being actively aged at 177 °C. The lignite could not withstand the high-temperature drilling environment of 170 °C. The inherent structural deficiencies of traditional humic acids limit the excellent performance of humic acid-based drilling fluid additives. To overcome these limitations, humic acids have been modified to improve their properties.

The molecular structure of CP is distinguished by its dense arrangement of aromatic hydrocarbon and alkyl substituents. This unique configuration contributes to its exceptional chemical properties and enhanced performance, surpassing conventional humic acids. Zhang et al. (2016) affixed a sulfur phenolic resin to lignite to produce a lignite graft polymer that displays a reduction in American Petroleum Institute (API) fluid loss (FL_{API}) and dispersion properties in water bentonite mud. Nevertheless, this product's drawback is an excessive increase in the viscosity of the drilling fluid, even as it reduced the FL_{API}. The experimental process produced harmful gases like SO_2 and SO_3, significantly contaminating the environment. The molecular structure of CP is characterized by its distinctive arrangement of a dense, aromatic hydrocarbon core accompanied by alkyl substituents. This exceptional configuration potentially imparts CP with remarkable resistance to elevated temperatures and salinity levels (Sun et al., 2020). When employed as a raw material for humate salt production, it can be inferred that CP holds promising potential for exhibiting distinctive properties and effects as a drilling additive with high-temperature and salt resistance capabilities. Consequently, the imperative need arises to develop CP-based drilling additives.

This study synthesized a novel polycondensate molecular structure using HA-K obtained from the low-temperature pyrolysis of CP. The research investigated the impact of anti-warming and viscosity reduction in high-temperature and high-pressure drilling environments, comparing the new structure with commercial HA-K. The Graft CP-HA-K polymer exhibited superior anti-temperature and viscosity-reducing properties compared to the commercial HA-K polymer. This study has significant implications for reducing drilling costs and dependence on conventional petrochemical products, leading to decreased environmental contamination. These findings are anticipated to provide substantial economic and ecological benefits to the drilling industry while introducing an innovative approach to utilizing CP resources.

2. Experimental

2.1. Material

The reagents used and their purity are as follows: potassium hydroxide (KOH, AR, 99%), polyacrylonitrile (PAN, AR, 99%), sodium hydroxide (NaOH, AR, 99%), urea ($CO(NH_2)_2$, AR, 99%), formaldehyde (HCHO, AR, 99%), phenol (C_6H_6O, AR, 99%), acrylamide (AAM, AR, 99%), anhydrous sodium carbonate (Na_2CO_3, AR, 99%), sodium chloride (NaCl, AR, 99%), calcium chloride ($CaCl_2$, AR, 99%), ferric chloride ($FeCl_3·6H_2O$, AR, 99%). The above reagents are purchased from Shanghai Aladdin Biochemical Technology Co. Bentonite is sodium bentonite provided by Hami Shentu Science and Technology Co., Ltd., CP is supplied by Hebei Fengtai Energy Science and Technology Co, and PAC-LV is supplied by Hebei HaiDrill Petrochemicals Co.

2.2. Characterization and analysis

The synthesized C-HA-K, CP-HA-K, Graft C-HA-K polymer, and Graft CP-HA-K polymer are observed by emission field scanning electron microscopy (SEM) on a Hitachi SU-8000 field emission electron microscope with an operating voltage of 20 kV. Fourier infrared spectroscopy (FTIR, Thermo Scientific Nicolet 10, Germany) analyzed the functional group compositions of the samples in the range of 4000–400 cm^{-1}. Solid-state nuclear magnetic resonance spectroscopy (NMR, BRUKER AVANCE NEO 400WB, USA) analyzed the samples' available group structure and composition. The microscopic particle size of the pieces is examined by a laser particle sizer (Mastersizer, 2000/3000, USA). The mass change of the copolymers from 30 to 800 °C is recorded with a Thermal Gravimetric Analyzer (Germany) under air protection at 5 °C·min^{-1}. The zeta potential of the samples and the sample-treated bentonite dispersions are determined using a zeta potential analyzer (Zetasizer Nano, UK).

FL_{API} at ambient and medium pressure is measured using an SD3

filter unit (Shandong Meike Instrument Co., Ltd., China, Shandong Meike Instrument Co., Ltd., China). High Temperature High Pressure Fluid Loss (FL_{HTHP}) is measured using a GGS71 high-temperature and high-pressure filtration unit at 3.5 MPa (Shandong Meike Instrument Co., Ltd., China). It is advisable to maintain consistent spacing between sentences throughout the entire document. This manuscript should adhere to the following guidelines.

2.3. Catalytic preparation of CP-HA-K

First, the CP samples are crushed to pass through a 100-mesh sieve and dried at 80 °C. Then, 2 g of pre-treated CP and Fe_2O_3 are accurately weighed and mixed in a ratio of 1: X (X represents the mass fraction of iron in iron (III) oxide, $X = 0.5\%, 1\%, 1.5\%, 2.0\%, 2.5\%, 3.0\%$). Subsequently, a specific amount of KOH (0.1, 0.2, 0.3, 0.4, 0.5, 0.6 g) is added and mixed. After being heated with air at a set temperature (175, 200, 225, 250, 275, 300 °C) for a determined time frame (80, 100, 120, 140, 160, 180 min), the CP is quickly cooled, filtered, and dried at a temperature of 80 °C to attain CP-HA-K. The yield of CP-HA-K is calculated using Eq. (1):

$$y = \frac{m}{m_1} \times 100\% \tag{1}$$

Formula: y-Yield of CP-HA-K, %;
m-Mass of HA-K obtained, g;
m_1-Mass of CP, g.

2.4. Preparation and characterization of Graft HA-K polymer

Graft HA-K polymers are prepared by free radical polymerization (Morita et al., 2003). In a typical experiment, a certain amount of Na-HPAN, urea, formaldehyde, phenol, and AAM (Fig. 1) are sequentially added to the HA-K solution prepared under the above optimal conditions and reacted at 70 °C for 0.5 h, respectively. Then, the solution is moved to a polytetrafluoroethylene liner and subjected to a reaction at 150 °C for 3 h. The answer is cooled after the response, and the resulting product is obtained after drying at 80 °C. The orthogonal experiments for synthesizing Graft CP-HA-K polymer are shown in Table 1.

Table 1
The orthogonal experiment table of Graft CP-HA-K polymer.

Experiment	Phenol, g	Methanal, mL	Urea, g	Na-HPAN, g	AAM, g
1	0.0	10.0	0.0	0.0	0.0
2	0.0	12.0	5.0	4.0	0.5
3	0.0	15.0	10.0	7.0	1.0
4	0.0	20.0	16.0	10.0	2.0
5	4.0	10.0	5.0	7.0	2.0
6	4.0	12.0	0.0	10.0	1.0
7	4.0	15.0	16.0	0.0	0.5
8	4.0	20.0	10.0	4.0	0.0
9	6.0	10.0	10.0	10.0	0.5
10	6.0	12.0	16.0	7.0	0.0
11	6.0	15.0	0.0	4.0	2.0
12	6.0	20.0	5.0	0.0	1.0
13	8.0	10.0	16.0	4.0	1.0
14	8.0	12.0	10.0	0.0	2.0
15	8.0	15.0	5.0	10.0	0.0
16	8.0	20.0	0.0	7.0	0.5

2.5. Effect of viscosity reducer addition on rheological parameters of drilling fluids

Add 0–4 wt% (0, 0.5, 1, 2, 3, 4 wt%) of Graft HA-K polymer to the 4% fresh water-based mud after 24 h of conditioning. Then, test the rheological parameters and the amount of FL_{API} before and after aging for 16 h at 120 °C with high-speed mixing at 10000 r·min^{-1} for 20 min to identify the optimal dosage of a viscosity reducer.

2.6. Aging temperature test

To determine the optimal aging temperature of a viscosity-reducing agent, add the appropriate amount of Graft HA-K polymer condensate to a 4% freshwater mud and let it sit for 24 h. Following this, let the mixture sit at varying temperatures (80, 90, 100, 110, 120, 130, 140, 150, 160, 170, 180 °C) for 16 h after high-speed stirring at 10000 r·min^{-1} for 20 min. Measure the rheological parameter and the amount of FL_{API} of the drilling fluid before and after aging.

2.7. Salt and calcium resistance test

NaCl (0, 1, 2.5, 5, 10, and 20 wt%) or $CaCl_2$ (0, 0.1, 0.25, 0.5, 0.75, and 1 wt%) is introduced into the 2.0% freshwater mud, which is

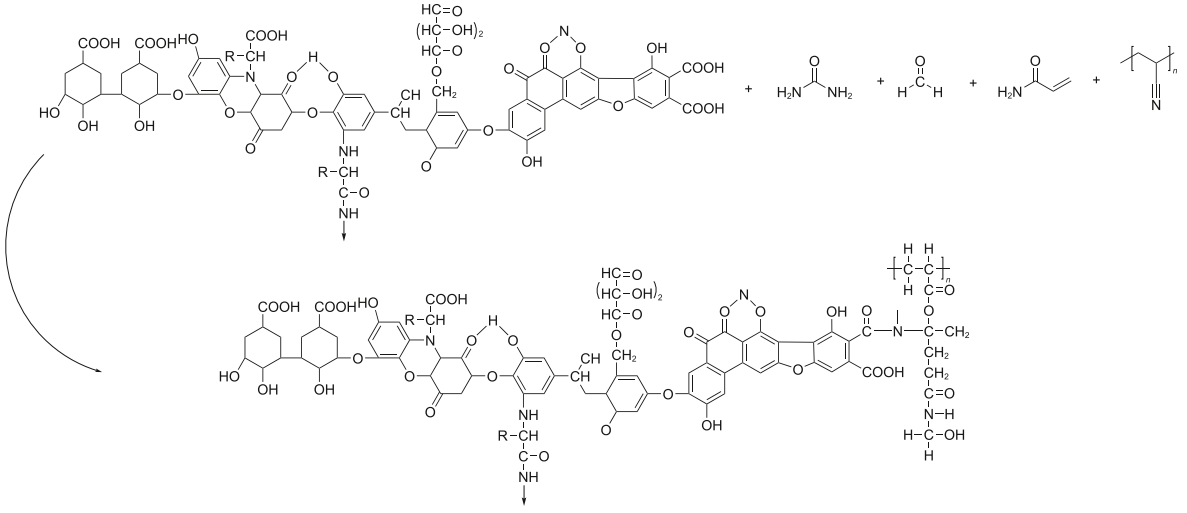

Fig. 1. Synthesis route of the polymer.

subsequently stored in a sealed container for 24 h. An optimal amount of Graft CP-HA-K polymer and CP-HA-K is separately added to this mixture, then aged for 16 h at the optimum aging temperature with high-speed mixing at 10000 $r \cdot min^{-1}$ for 20 min. After being aged for 16 h at the optimal temperature, the drilling fluid's rheological parameters and FL_{API} are measured before and after aging to ascertain the viscosity reducer's anti-salt and anti-calcium properties.

3. Results and discussion

3.1. Optimal preparation conditions for CP-HA-K

The impact of catalyst Fe_2O_3 dosage, KOH dosage, roasting temperature, and roasting time on CP-HA-K yield is presented in Fig. 2(a)–(d), respectively. As illustrated in Fig. 2, the most favorable conditions for the catalytic preparation of CP-HA-K are 1% catalyst dosage (as a percentage of CP dosage), 30% KOH dosage (as a percentage of CP dosage), a reaction temperature of 250 °C and a reaction time of 2 h, which resulted in a maximum yield of CP-HA-K of 39.58%.

3.2. Comparison of viscosity reduction rates of Graft CP-HA-K polymer

Let *T*, *AV*, *PV*, *YP*, and *VR* represent temperature, apparent viscosity, plastic viscosity, yield point, and viscosity reduction, respectively. Let *G*10″ represent the gel strength when the drilling fluid is allowed to stand for 10 s at 3 $r \cdot min^{-1}$, and *G*10′ represent the gel strength when the drilling fluid is allowed to stand for 10 min at 3 $r \cdot min^{-1}$. Table 2 exhibits the plastic viscosity reduction capabilities and rheological properties of WBDF with varied viscosity reduction amounts before and after thermal aging examinations. The rheological model is presumed to be the Bingham model based on the drilling fluid's rheological parameters (Zhao et al., 2008). At ambient temperature, the *VR* of Graft CP-HA-K polymer is 58.62%, 55.17% more than the reduction offered by commercial HA-K. After being aged at 120 °C, the Graft CP-HA-K polymer exhibits a significantly higher reduction in viscosity compared to C-HA-K, reaching a rate of 63.16%. Experiment 4, which has undergone modification, showed the highest viscosity reduction rate of 58.62% before aging, with the most considerable effect. After aging, the viscosity reduction rate of experiment 4 remains the highest at 63.16% with the most pronounced effect. Hence, the fourth modified experiment, Graft CP-HA-K polymer, is deemed the optimal modified program.

3.3. Characterization of Graft CP-HA-K polymer

Fig. 3(a)–(d) presents SEM images of C-HA-K, CP-HA-K, Graft C-HA-K polymer, and Graft CP-HA-K Polymer, respectively. The pictures depicted in Fig. 3 reveal that both C-HA-K and CP-HA-K exhibited large-particle lumpy structures. Furthermore, Graft C-HA-K polymer has a loose surface and visible laminar structure at its edges. Similarly, Graft CP-HA-K polymer forms a large-particle accumulation that reduces densification, thereby creating a favorable pathway for the circulation of drilling fluids. Fig. 3(e) displays the particle size distribution of CP-HA-K, Graft C-HA-K polymer, and Graft CP-HA-K polymer. As depicted in Fig. 3(e), CP-HA-K has a broader particle size distribution, with an average particle size of 614.4 nm. On the other hand, Graft C-HA-K polymer and Graft CP-HA-K polymer have average particle sizes of 552.1 and 538.7 nm, respectively. Notably, Graft CP-HA-K polymer has a smaller particle size than Graft C-HA-K polymer. The smaller particle size of the polymer disrupts the flocculating mesh structure of the clay particles, which disperses the clay particles and reduces viscosity. The results are consistent with the SEM results.

Fig. 4(a) illustrates the thermogravimetric curves of the Graft C-HA-K polymer, Graft CP-HA-K polymer, and CP-HA-K (Liu et al., 2018). According to Fig. 4(a), the weight loss of the products starts at a temperature range of 30–177.39 °C during the first stage. The TGA curve also demonstrates a progressive decrease, with a 21.19% mass loss, suggesting that the synthesized products' mass lowers due to thermal absorption. The carboxylic acids and amides present in the synthesized products indicate the presence of many hydrophilic groups. When the drilling fluid's water molecules

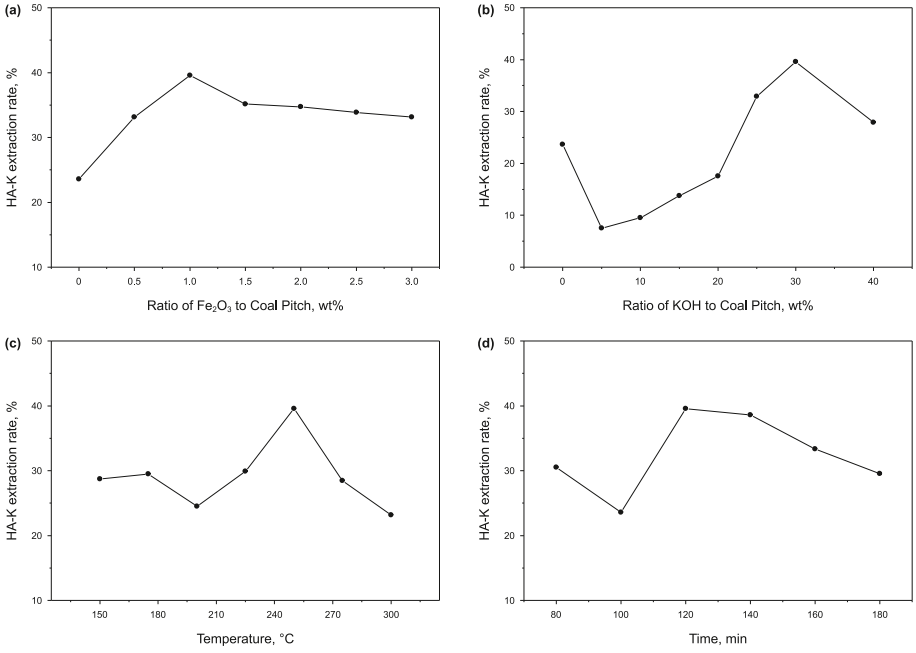

Fig. 2. Effects of **(a)** catalyst dosage, **(b)** KOH dosage, **(c)** roasting temperature, and **(d)** roasting time on the extraction rate of CP-HA-K.

Table 2
Rheological parameters of various fluid formulations.

Fluid formulation	*T*, °C	*AV*, mPa·s	*PV*, mPa·s	*G*10″, Pa	*G*10′, Pa	*YP*, Pa	*VR*, %
Base fluid	RT	22.0	6.0	10.5	12	16.0	–
	120	17.5	9.0	7.0	8.0	8.5	–
C-HA-K fluid	RT	23.0	14.0	10.5	11.5	9.0	3.45
	120	11.0	7.0	5.5	6.0	4.0	42.12
CP-HA-K fluid	RT	17.5	8.0	9.0	10.0	9.5	24.14
	120	10.0	7.0	3.0	4.0	3.0	57.89
1 fluid	RT	20.0	8.0	10.5	11.0	12.0	10.34
	120	12.0	7.0	6.0	7.5	5.0	47.37
2 fluid	RT	17	7	7.5	8.0	8.5	34.48
	120	13	9	5.0	6.5	4	47.37
3 fluid	RT	14	6	7.0	8.0	8	55.17
	120	8.5	6	2.0	3.0	2.5	61.42
4 fluid	RT	14	8	6.0	7.0	6	58.62
	120	10.5	8	1.5	3.0	2.5	63.16
5 fluid	RT	14	8	6.5	7.0	6	51.72
	120	13	9	5.0	6.0	4	47.37
6 fluid	RT	13	7	6.5	7.5	6	51.72
	120	8.5	8	1.0	2.0	0.5	62.84
7 fluid	RT	22.5	5	11.0	12.5	17.5	–
	120	14.5	7	7.0	8.0	7.5	15.79
8 fluid	RT	27	12	10.0	11.5	15	–
	120	11.5	9	1.5	3.0	2.5	47.37
9 fluid	RT	18	13	6.0	7.5	5	51.72
	120	10	8	1.0	2.5	2	63.16
10 fluid	RT	20	13	6.5	8.0	7	27.59
	120	10	9	1.5	2.0	1	63.16
11 fluid	RT	22	9	10.5	11.0	13	10.34
	120	10	7	2.0	3.5	3	63.16
12 fluid	RT	26	11	10.5	12.0	15	–
	120	16	7	8.0	9.5	9	10.53
13 fluid	RT	24	8	10.5	12.0	16	–
	120	10.5	7	2.0	3.5	3.5	52.63
14 fluid	RT	26	11	10.0	11.5	15	–
	120	15	5	8.5	10.0	10	–
15 fluid	RT	19	7	9.0	10.5	12	20.69
	120	8.5	7	0.5	1.0	1.5	60.28
16 fluid	RT	21	3	12.0	14.0	18	–
	120	11	8	1.0	2.5	2	57.89

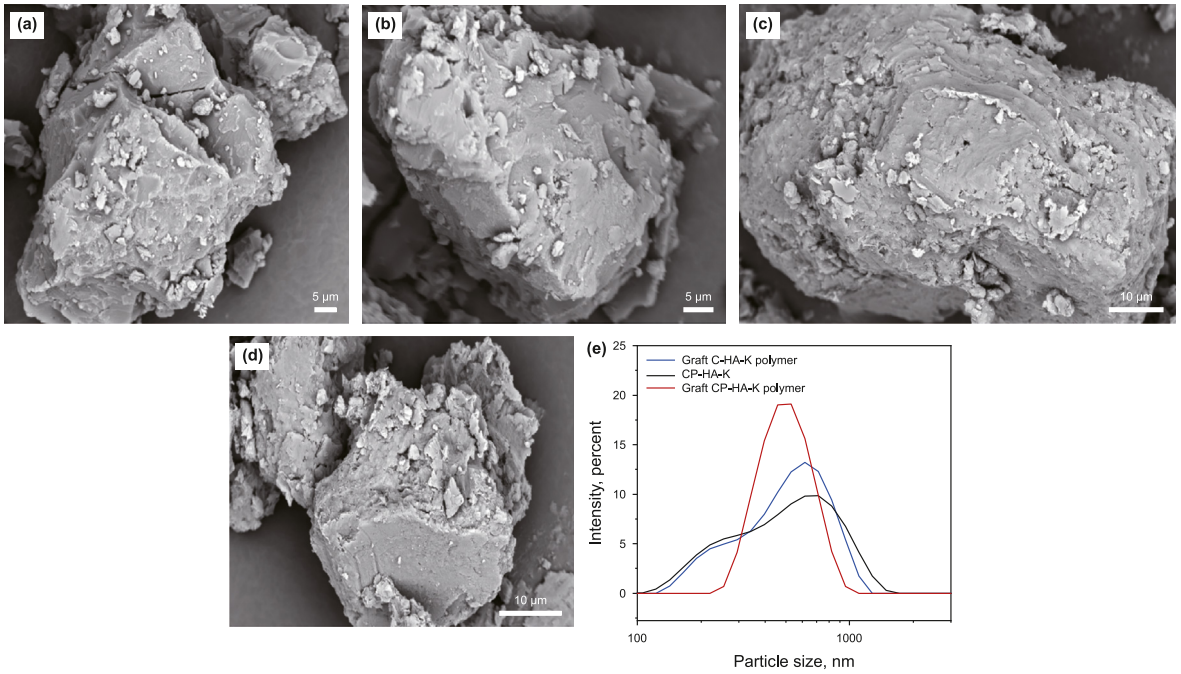

Fig. 3. The SEM images of **(a)** C-HA-K, **(b)** CP-HA-K, **(c)** Graft C-HA-K polymer, **(d)** Graft CP-HA-K polymer, and **(e)** Particle size distribution of C-HA-K, CP-HA-K, Graft C-HA-K polymer, and Graft CP-HA-K polymer.

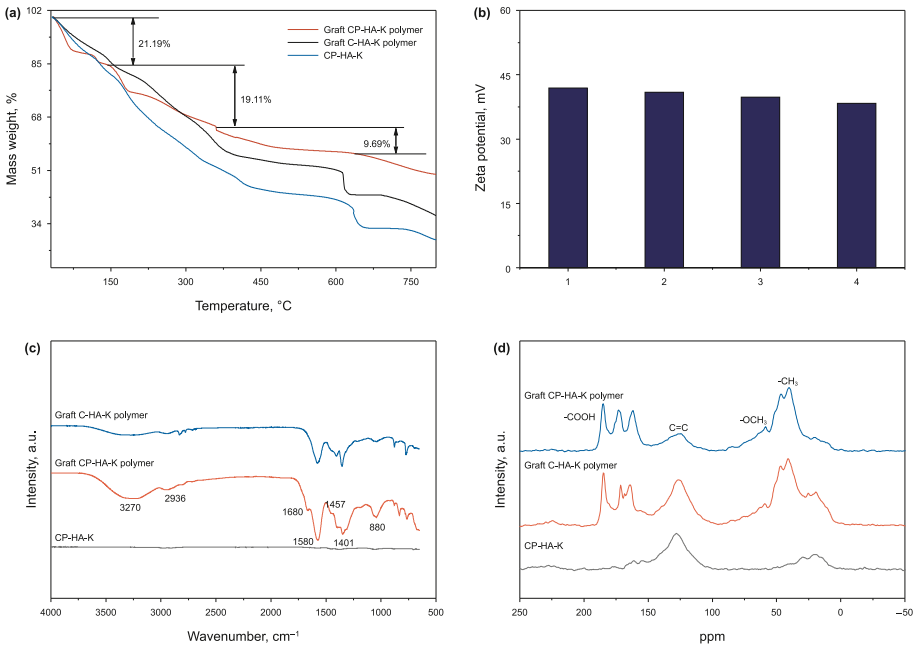

Fig. 4. **(a)** Thermogravimetric analysis (TGA) of the Graft C-HA-K polymer, Graft CP-HA-K polymer, and CP-HA-K; **(b)** Absolute values of Zeta potentials for products 1, 2, 3, 4 (1 indicates WBDF, 2 indicates CP-HA-K, 3 means Graft C-HA-K polymer, 4 exhibits Graft CP-HA-K polymer); **(c)** Fourier infrared spectrogram of Graft C-HA-K polymer, Graft CP-HA-K polymer, and CP-HA-K; **(d)** Nuclear magnetic resonance spectrogram of Graft C-HA-K polymer, Graft CP-HA-K polymer, and CP-HA-K.

contact the synthesized material, they adsorb onto the derivative's hydrophilic groups. The product's weight decreases as the temperature rises gradually. When the heating temperature exceeds 177.39 °C, the amide group and carboxylic acid absorb significant heat and initiate decomposing and volatilizing. During this stage, the TGA curve shows a significant decline, with a remarkable increase in mass loss resulting in a 19.11% reduction. When the temperature surpasses 443 °C, the amide group starts to decompose, leading to a continued downward trend of the TGA curve and ending with a weight reduction of 9.69%. The above findings can be rationalized by exposing the product to considerable heat, breaking the center and side chains in the molecular structure, resulting in the product's melting and the evaporation of oxygen. During the final phase of product weight loss, the TG curve remains relatively stable, suggesting that the product has been carbonized. As a result, the evaporation of carbon causes a continuous deterioration in product quality. The comparison of TGA curves for Graft C-HA-K polymer and CP-HA-K reveals that Graft CP-HA-K polymer can withstand a high temperature of 177.39 °C, demonstrating a robust product structure resistant to thermal degradation. Meanwhile, Graft C-HA-K polymer and CP-HA-K experience notable thermal degradation before reaching 612.55 and 613.93 °C, respectively, while the weight of the resulting products decreases continuously. The above results indicate that both materials are unable to withstand high-temperature degradation.

Fig. 4(b) displays the absolute value deviation in zeta potential for these additives. From Fig. 4(b), it can be observed that the potentials of Graft CP-HA-K polymer, Graft C-HA-K polymer, and CP-HA-K are −38.3, −39.8, and −40.9 mV, respectively. The Graft CP-HA-K polymer has a higher potential value, which can increase the zeta potential of the bentonite particles and thus increase the repulsive force between solid particles. This leads to the instability of the clay structure and a decrease in the viscosity of the drilling mud cake.

Fig. 4(c)–(d) display the infrared and solid-state NMR spectra for Graft C-HA-K polymer, Graft CP-HA-K polymer, and CP-HA-K, respectively. It is evident from Fig. 4(c) that the positions of the IR peaks for the different HA-K polymers are nearly identical, demonstrating that the classes of the contained functional groups have similar properties. 3270 cm^{-1} corresponds to the absorption peak of the N—H stretching vibration, whereas 2936 cm^{-1} corresponds to the C—H stretching vibration of —CH, and 1682 cm^{-1} represents the amide group absorption peak. The height at 1581 cm^{-1} corresponds to the stretching vibration of C=C in aromatic rings, the rise near 1457 cm^{-1} represents the stretching vibration of C—N, the peak at 1401 cm^{-1} corresponds to the absorption peak of —COOH in condensates, and the increase at 880 cm^{-1} reaches to the out-of-plane bending vibration of C—H in aromatics. The results indicate the presence of all five monomers in the resulting copolymerized electrolyte, demonstrating the successful synthesis of the condensate.

^{13}C-NMR is a valuable technique for evaluating the organic matter composition of condensates. These categories allow for a comprehensive analysis of the sample's chemical structure. The solid-state NMR carbon spectra can be divided into four chemical regions, namely aliphatic carbon (0–50 ppm), oxygenated aliphatic carbon (50–100 ppm), aromatic carbon (100–160 ppm), and carboxyl/carbonyl carbon (160–220 ppm). Fig. 4(d) illustrates that the peak centered at 30 ppm originates from aliphatic $-CH_3$, while the signals at 56 and 130 ppm can be attributed to aromatic methoxy $-OCH_3$ and unsaturated carbon (Srungavarapu et al., 2018). The peaks in the chemical shift range of 165–190 ppm are characteristic peaks of the carboxyl group. The mountains in this range appear more intense for the Graft CP-HA-K polymer in Fig. 4(d), indicating a higher carboxyl content. The above results are consistent with the results of infrared spectrogram analysis, confirming that the molecular structure of the target product is following the pre-design.

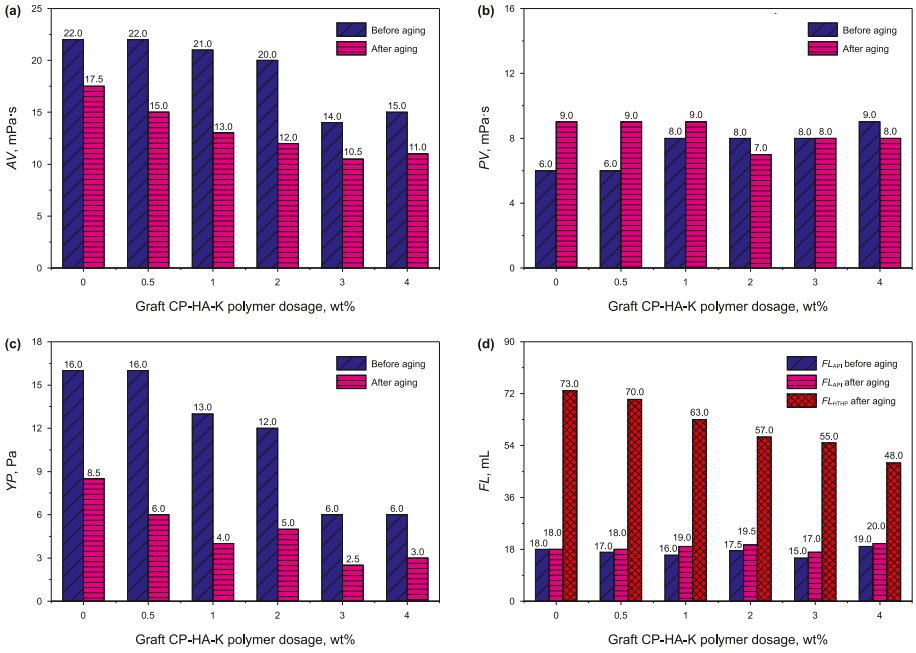

Fig. 5. Values of **(a)** *AV*, **(b)** *PV*, **(c)** *YP*, and **(d)** FL_{API} before and after aging at 120 °C for 16 h containing the Graft HA-K polymer of different concentrations.

3.4. Effect of Graft CP-HA-K polymer addition on WBDF rheological properties

Fig. 5 depicts the rheological characteristics and FL_{API} of WBDF containing different concentrations of Graft HA-K polymer after aging for 16 h at 120 °C. The results show that the viscosity of Graft HA-K polymer initially increases and then decreases as the polymer concentration increased from 0.5 to 4.0 wt%. In addition, a decrease in filtrate loss is observed. At a concentration of 3.0 wt% Graft CP-HA-K polymer, the *AV* of WBDF decreases from 17.5 to 10.5 mPa·s, with a gradual reduction in liquid loss. Table 1 shows a 58.62% decrease in viscosity before aging at 120 °C for 16 h, and a 63.16% decrease after aging, indicating the potential of Graft HA-K polymer to reduce the viscosity of WBDF at 120 °C. The FL_{API} values of the aged WBDF are 18.0 and 73 mL, which are within the oil and gas industry standard SY/T 7626-2021. These results suggest that the optimal percentage of Graft CP-HA-K polymer is 3.0 wt%. Therefore, we test the best dosages of Graft CP-HA-K polymer, which are 3.0 wt%, for their resistance to aging temperature and salt.

3.5. Effect of aging temperature on the rheological properties of Graft CP-HA-K Polymer

Table S14 displays the rheological parameters of different fluid formulations subjected to varying aging temperatures. The products Graft C-HA-K polymer and Graft CP-HA-K polymer exhibit a decrease in *AV*, *PV*, and *YP* as the temperature increases. Nonetheless, even after undergoing an aging process at 170 °C for 16 h, the *AV* value of the Graft CP-HA-K polymer remains at 10.5 mPa·s. The *AV* value of the Graft C-HA-K polymer is reduced to 10.0 mPa·s after 16 h of aging at 100 °C. Hence, the temperature resistance of the Graft CP-HA-K polymer is superior to that of the Graft C-HA-K polymer. This phenomenon can be explained by the gradual thermal degradation of the main chain of the copolymer molecule as the temperature increases. The hydrolysis of the amide groups on the side chains leads to a higher frequency of chain breaks in the copolymer, significantly reducing molecular weight, leading to a reduction in the viscosity of the copolymer in an aqueous solution at the macroscopic level, and ultimately losing its ability to minimize leaching. At high temperatures, the solvation film surrounding the molecular chain of the polymer is disrupted. As a result, the entropy of the CP-HA-K polymer in the surrounding environment increases, leading to an increase in the molecular chain length. This increase in chain length consequently reduces the viscosity of the aqueous polymer solution.

Graft CP-HA-K polymer is modified with formaldehyde, urea, and sodium hydrolyzed polyacrylonitrile. It contains a large number of amine, hydroxyl, and amide groups, which effectively increase the length of the polymer's carbon chain for high-temperature and high-salt stability. Simultaneously, the molecular groups linking the side chains of humic acid contain carbon-carbon and carbon-nitrogen bonds. These bonds enhance the hydration and adsorption functional groups of the polymer, making it more resistant to high-temperature and high-salt environment (Shumaker et al., 2012).

3.6. Effect of salt resistance on the rheological properties of Graft CP-HA-K Polymer

Insufficient resistance of the treatment agent to salt erosion during oil drilling may lead to the collapse of the hole wall (Shu and Ma, 2016). Fig. 6 presents the rheological parameters of different fluid formulations under varying NaCl concentrations. The viscosity of WBDF rises initially and then falls after NaCl addition. The *AV*, *PV*, and *YP* values of the drilling fluids show minor changes at room temperature and after being aging at 120 °C with 1–20 wt% NaCl. The aged drilling fluids' *AV*, *PV*, and *YP* values slightly change at room temperature and 120 °C. At a temperature of 120 °C, the *AV* and *PV* values of the previous drilling fluids decreased from 10.5 and 8.0 to 6.0 and 3.0 mPa·s, respectively, which complies with the oil and gas industry standard SY/T 7626-2021. This implies that the viscosity reducer can resist drilling fluids with a NaCl concentration of up to 8000 $mg \cdot L^{-1}$. Its resistance to salt intrusion is found to be exceptional.

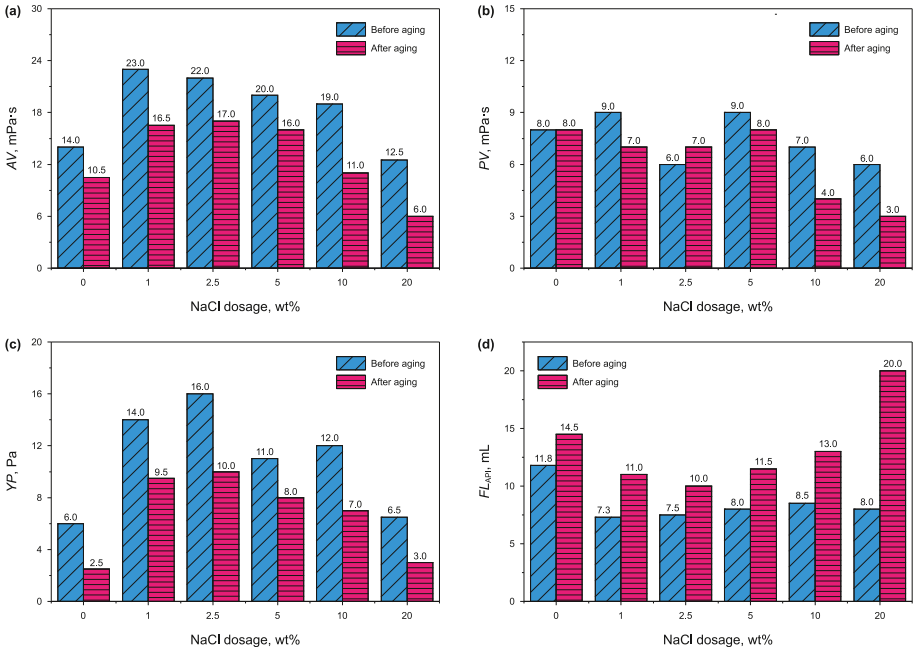

Fig. 6. Effect of sodium chloride on the **(a)** *AV*, **(b)** *PV*, **(c)** *YP*, and **(d)** FL_{API} values of fluid with 3.0% polymer additive before and after aging at 120 °C for 16 h.

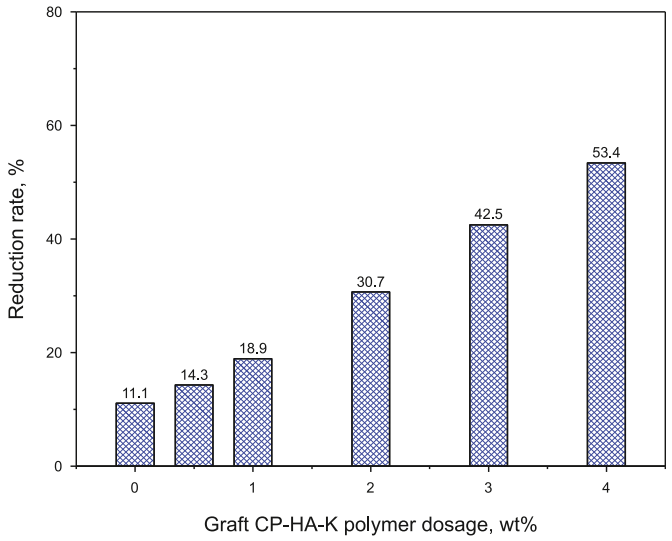

Fig. 7. Reduction of coefficient of friction at different Graft CP-HA-K polymer concentrations in a 4% freshwater-based mud.

3.7. Testing of mud lubrication properties

Friction coefficients are measured for various concentrations of Graft CP-HA-K polymer. The experimental results are presented in Fig. 7. The reduction in friction coefficient increases from 11.1% to 53.0% as the polymer concentration increases from 0% to 4.0%. Graphite, a commonly used solid lubricant at a concentration of 1.0%, reduces the friction coefficient by 47.6%. While Graft CP-HA-K polymer may not perform as well as special-purpose lubricants, it can significantly improve the lubricity of drilling mud. This is due to Graft CP-HA-K polymer's ability to enhance interfacial smoothness, isolate direct contact between the wellbore and drill string, and transform the friction between them into crystal layer sliding, ultimately reducing friction (Chen et al., 2015; Kong et al., 2017).

3.8. Anti-salt and viscosity reduction working mechanism of Graft CP-HA-K polymer

Fig. 8(a)–(f) displays SEM images of the filter cake after aging with diverse additives. Fig. 8 exhibits a clear "reticulation" structure in WBDF devoid of NaCl contamination. The introduction of Graft CP-HA-K polymer breaks down the mesh structure of the drilling fluid and diminishes the viscosity of WBDF. The formation of hydroxyl groups and the breakdown of metabolites are coupled phenomena that result in the polymerization of bentonite at high temperatures. Such polymerization causes the flocculation of bentonite particles into a blocky structure, ultimately reducing WBDF viscosity.

Fig. 8(g) illustrates the particle size distribution for various additives, while Fig. 8(h) displays the absolute value deviation in zeta potential for these additives. The images show that adding Graft CP-HA-K polymer and Graft C-HA-K polymer reduces the average particle size. The images show that adding Graft CP-HA-K polymer and Graft C-HA-K polymer reduces the average particle size of bentonite to 579 and 833.7 nm, respectively. Nonetheless, Graft CP-HA-K polymer has a smaller particle size and can impede the drilling fluid's reticulation to create smaller dispersed particles. The findings align with those observed in SEM images of the polymerized samples. Furthermore, the Graft CP-HA-K polymer, which is a viscosity reducer, has been modified with Methanal, Urea, Na-HPAN, and AAM. This modification results in the polymer having a significant amount of amide, hydroxyl, and amine groups, which improve its water solubility and thermal stability. Fig. 8(h) illustrates that the Graft CP-HA-K polymer increased the electrical potential of the drilling fluid from −41.5 to −34.6 mV. This increase is due to the significant adsorption of hydroxyl and amide groups on the surface of the bentonite particles, which effectively increase the electrostatic repulsion between the solid particles and the thickness of the hydration film. As a result, the electrostatic repulsion between bentonite particles is maximized, causing the clay structure to destabilize and ultimately reducing the overall viscosity of the drilling fluid.

Fig. 9 illustrates pictures of mud with various additives.

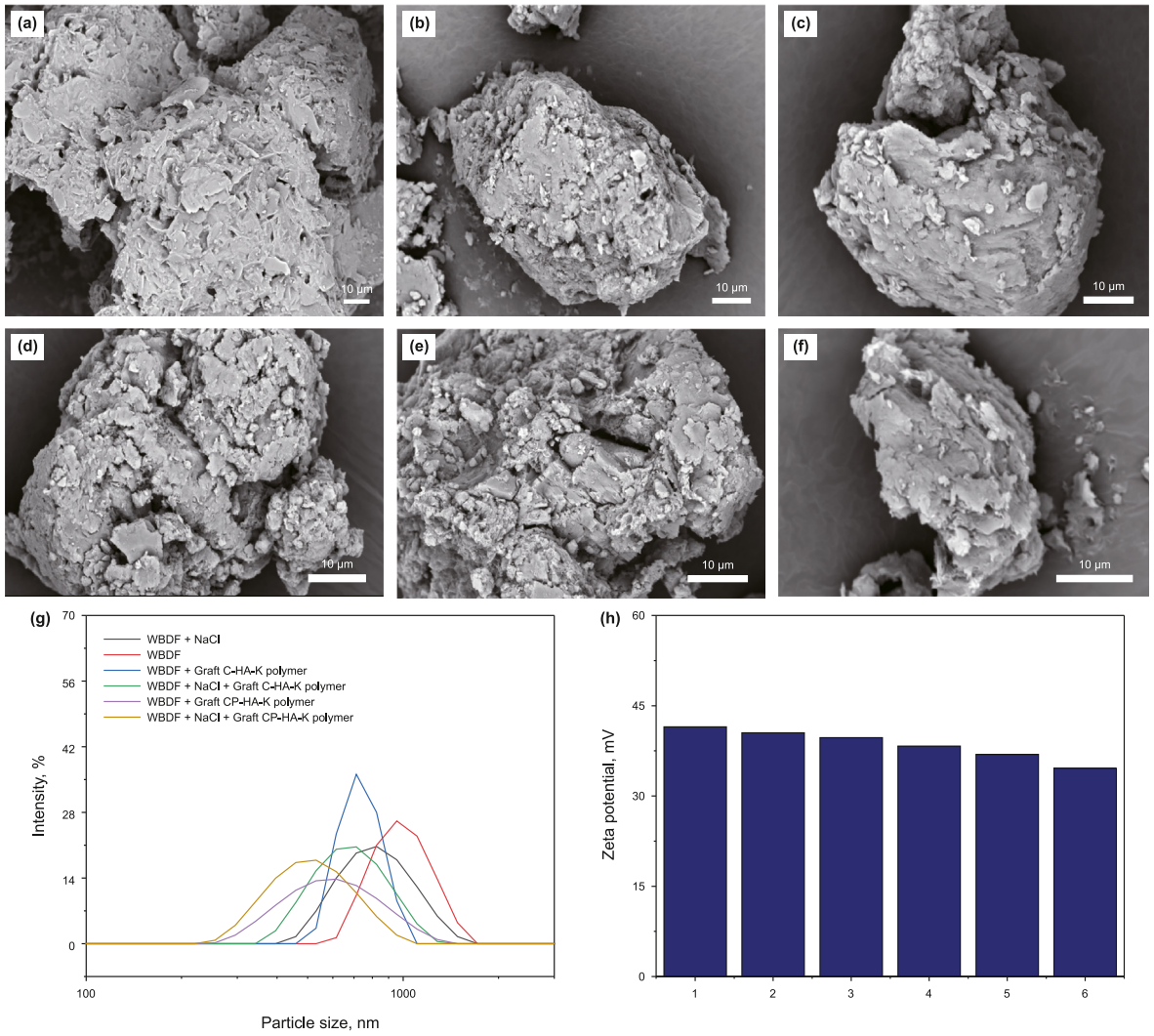

Fig. 8. The SEM images of **(a)** WBDF, **(b)** WBDF + NaCl, **(c)** WBDF + Graft C-HA-K polymer, **(d)** WBDF + NaCl + Graft C-HA-K polymer, **(e)** WBDF + Graft CP-HA-K polymer, and **(f)** WBDF + NaCl + Graft CP-HA-K polymer after aging at 120 °C for 16 h; **(g)** Particle size distribution of WBDF, WBDF + NaCl, WBDF + Graft C-HA-K polymer, WBDF + NaCl + Graft C-HA-K polymer, WBDF + Graft CP-HA-K polymer, and WBDF + NaCl + Graft CP-HA-K polymer after aging at 120 °C for 16 h; **(h)** Effect of products 1, 2, 3, 4, 5 and 6 on the absolute value of the zeta potential (1 indicates WBDF, 2 indicates WBDF + NaCl, 3 means WBDF + Graft C-HA-K polymer, 4 exhibits WBDF + Graft CP-HA-K polymer, 5 indicates WBDF + NaCl + Graft C-HA-K polymer, 6 indicates WBDF + NaCl + Graft CP-HA-K polymer).

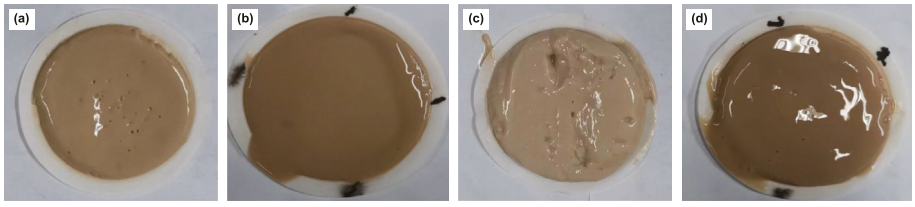

Fig. 9. The mud pictures of **(a)** WBDF, **(b)** WBDF + 3 wt% Graft CP-HA-K polymer, **(c)** WBDF + 10 wt% NaCl, and **(d)** WBDF + 10 wt% NaCl + 3 wt% Graft CP-HA-K polymer.

Fig. 9(a)–(c) indicate that the clay particles in the WBDF and 10 wt% NaCl-added mud are loosely packed, with visible holes and microcracks on the surface of the mud cake. However, the introduction of Graft CP-HA-K polymer can improve this. Fig. 9(b)–(d) demonstrate that the presence of Graft CP-HA-K polymer leads to a better distribution of clay particles in the drilling fluid system, promoting tight packing between particles. The denser packing effect has a significant impact on reducing the formation of holes and microfractures, as well as lowering the filtration loss of the mud.

Table 3
Rheological parameters of Graft CP-HA-K polymer repeatability experiments.

Cycle times	*AV*, mPa·s	*PV*, mPa·s	*YP*, Pa	*VR*, %
0	10.5	8.0	2.5	63.16
1	12.0	8.0	4.0	40.23
2	15.5	9.0	6.5	31.05
3	16.0	9.0	7.0	8.79
4	18.0	9.5	8.5	–

Table 4
Scale-up experiments for synthetic processes.

Experiment	Methanal, mL	Urea, g	Na-HPAN, g	AAM, g	CP, g	Graft CP-HA-K polymer, g
1	20.0	16.0	10.0	2.0	2.0	5.92
2	100.0	80.0	50.0	10.0	10.0	26.32
3	200.0	160.0	100.0	20.0	20.0	51.73

3.9. Reproducibility and scale-up experiments of synthetic processes

Table 3 shows the results of several replicate tests carried out on the Graft CP-HA-K polymer. As shown in the table, as the number of replicates increases, the *AV* of the mud gradually increases and the viscosity-reducing property decreases. This indicates that the *VR* effect of the Graft CP-HA-K polymer is gradually decreasing. When the experiment is carried out four times, the polymer essentially loses its viscosity-reducing ability. In summary, the Graft CP-HA-K polymer shows a certain degree of recyclability, resulting in reduced raw material requirements and lower production costs, thus providing economic benefits.

Table 4 presents data on the scaling-up experiment for the synthesis process. Based on Table 4, the yield of Graft CP-HA-K polymer increases proportionally with the increase in the proportion of raw materials.

4. Conclusions

In this study, a new humic acid-based anti-temperature and viscosity reducing agent is prepared from solid waste high-temperature CP low-temperature pyrolysis process, and a new humic acid-based anti-temperature and viscosity reducing agent is prepared by free radical polymerization in solution. The synthesized humic acid-based anti-temperature and anti-viscosity reducer has excellent properties of temperature resistance up to 177.39 °C. After adding the optimum amount of 3 wt% Graft CP-HA-K polymer, the polymer has salt point resistance up to 8000 mg L^{-1} and aging *VR* up to 63.16%. These properties are superior to those of commercial HA-K polycondensates. The experimental results demonstrate that the most favorable conditions for the catalytic preparation of CP-HA-K are 1 wt% catalyst dosage, 30 wt% KOH dosage, a reaction temperature of 250 °C, and a reaction time of 2 h, resulting in a maximum yield of CP-HA-K of 39.58%. It is also found that Graft CP-HA-K polymer could increase the length of the carbon chains, enhance the electrostatic repulsion on the surface of solid particles and disrupt the reticulation structure of the drilling fluid, thus realizing excellent anti-temperature and viscosity reduction performance. The novel humic acid-based anti-temperature viscosity reducer proposed in this study has significant advantages in maintaining the safety of drilling workover, expands the range of drilling fluid viscosity reducers, and has a broad application prospect. In future work, we will explore the relationship between material deformation and deformation rate under external forces so as to optimize the process parameters, improve the performance of the products, and reduce the production cost.

CRediT authorship contribution statement

Jing Tan: Writing – original draft. **Wei Zhang:** Formal analysis. **Xiu-Ling Yan:** Formal analysis. **Hao Zhou:** Formal analysis. **Sher Bahadar Khan:** Formal analysis. **Seitkhan Azat:** Formal analysis. **Shi-You Yan:** Formal analysis. **Hao-Jie Ma:** Formal analysis. **Xin-Tai Su:** Formal analysis.

Declaration of competing interest

The authors declare that they have no known competing financial interests or personal relationships that could have appeared to influence the work reported in this paper.

Acknowledgments

This work was supported by the Key R & D projects in Xinjiang (2022B01042). Research and Innovation Team Cultivation Plan of Yili Normal University (#CXZK2021002).

Appendix A. Supplementary data

Supplementary data to this article can be found online at https://doi.org/10.1016/j.petsci.2024.04.009.

References

Aguiar, N.O., Olivares, F.L., Novotny, E.H., et al., 2013. Bioactivity of humic acids isolated from vermicomposts at different maturation stages. Plant Soil 362 (1–2), 161–174. https://doi.org/10.1007/s11104-012-1277-5.

Apostolidou, C., Sarris, E., Georgakopoulos, A., 2022. Dynamic thermal aging of water-based drilling fluids with different types of low-rank coals as environmental friendly shear thinning additives. J. Petrol. Sci. Eng. 208, 109758. https://doi.org/10.1016/j.petrol.2021.109758.

Becattini, V., Motmans, T., Zappone, A., et al., 2017. Experimental investigation of the thermal and mechanical stability of rocks for high-temperature thermal-energy storage. Appl. Energy 203, 373–389. https://doi.org/10.1016/j.apenergy.2017.06.025.

Bennett, B., Larter, S.R., 2000. Polar non-hydrocarbon contaminants in reservoir core extracts. Geochem. Trans. 2000 (5), 1–4. https://doi.org/10.1039/b005237j.

Camp, E.R., Jordan, T.E., Hornbach, M.J., et al., 2018. A probabilistic application of oil and gas data for exploration stage geothermal reservoir assessment in the Appalachian Basin. Geothermics 71, 187–199. https://doi.org/10.1016/j.geothermics.2017.09.001.

Chang, X., Sun, J., Xu, Z., et al., 2019. A novel nano-lignin-based amphoteric copolymer as fluid-loss reducer in water-based drilling fluids. Colloids Surf. A Physicochem. Eng. Asp. 583, 123979. https://doi.org/10.1016/j.colsurfa.2019.123979.

Chen, Z., Liu, X., Liu, Y., et al., 2015. Ultrathin MoS_2 nanosheets with superior extreme pressure property as boundary lubricants. Sci. Rep. 5 (1), 12869. https://doi.org/10.1038/srep12869.

Da Câmara, P.C.F., Madruga, L.Y.C., Marques, N.D.N., et al., 2021. Evaluation of polymer/bentonite synergy on the properties of aqueous drilling fluids for high-temperature and high-pressure oil wells. J. Mol. Liq. 327, 114808. https://doi.org/10.1016/j.molliq.2020.114808.

De Melo, B.A.G., Motta, F.L., Santana, M.H.A., 2016. Humic acids: structural properties and multiple functionalities for novel technological developments. Mater. Sci. Eng. C 62, 967–974. https://doi.org/10.1016/j.msec.2015.12.001.

Doskočil, L., Burdíková-Szewieczková, J., Enev, V., et al., 2018. Spectral characterization and comparison of humic acids isolated from some European lignites. Fuel 213, 123–132. https://doi.org/10.1016/j.fuel.2017.10.114.

Doulia, D., Leodopoulos, C., Gimouhopoulos, K., et al., 2009. Adsorption of humic acid on acid-activated Greek bentonite. J. Colloid Interface Sci. 340 (2), 131–141. https://doi.org/10.1016/j.jcis.2009.07.028.

Fuentes-Audén, C., Sandoval, J.A., Jerez, A., et al., 2008. Evaluation of thermal and mechanical properties of recycled polyethylene modified bitumen. Polym. Test. 27 (8), 1005–1012. https://doi.org/10.1016/j.polymertesting.2008.09.006.

Ghosh, B., AlCheikh, I.M., Ghosh, D., et al., 2020. Development of hybrid drilling fluid and enzyme-acid precursor-based clean-up fluid for wells drilled with calcium carbonate-based drilling fluids. ACS Omega 5 (40), 25984–25992. https://doi.org/10.1021/acsomega.0c03436.

Kelessidis, V.C., Tsamantaki, C., Michalakis, A., et al., 2007. Greek lignites as additives for controlling filtration properties of water–bentonite suspensions at high temperatures. Fuel 86 (7–8), 1112–1121. https://doi.org/10.1016/j.fuel.2006.10.009.

Kong, L., Sun, J., Bao, Y., 2017. Preparation, characterization and tribological

mechanism of nanofluids. RSC Adv. 7 (21), 12599–12609. https://doi.org/10.1039/c6ra28243a.
Lei, Q., Xu, Y., Yang, Z., et al., 2021. Progress and development directions of stimulation techniques for ultra-deep oil and gas reservoirs. Petrol. Explor. Dev. 48 (1), 221–231. https://doi.org/10.1016/s1876-3804(21)60018-6.
Liu, L., Pu, X., Rong, K., et al., 2018. Comb-shaped copolymer as filtrate loss reducer for water-based drilling fluid. J. Appl. Polym. Sci. 135 (11), 45989. https://doi.org/10.1002/app.45989.
Luo, Z., Pei, J., Wang, L., et al., 2017. Influence of an ionic liquid on rheological and filtration properties of water-based drilling fluids at high temperatures. Appl. Clay Sci. 136, 96–102. https://doi.org/10.1016/j.clay.2016.11.015.
Mao, H., Qiu, Z., Shen, Z., et al., 2015. Hydrophobic associated polymer based silica nanoparticles composite with core–shell structure as a filtrate reducer for drilling fluid at utra-high temperature. J. Petrol. Sci. Eng. 129, 1–14. https://doi.org/10.1016/j.petrol.2015.03.003.
Mao, H., Yang, Y., Zhang, H., et al., 2020. Conceptual design and methodology for rheological control of water-based drilling fluids in ultra-high temperature and ultra-high pressure drilling applications. J. Petrol. Sci. Eng. 188, 106884. https://doi.org/10.1016/j.petrol.2019.106884.
Morita, K., Ebara, K., Shibasaki, Y., et al., 2003. New positive-type photosensitive polyimide having sulfo groups. Polymer 44 (20), 6235–6239. https://doi.org/10.1016/s0032-3861(03)00636-0.
Patrakov, Y.F., Schastlivtsev, E.L., Mandrov, G.A., 2010. Characterization of brown coal humic and fulvic acids by IR spectroscopy. Solid Fuel Chem. 44 (5), 293–298. https://doi.org/10.3103/s0361521910050022.
Proidakov, A.G., 2009. Humic acids from mechanically treated coals: a review. Soil Fuel Chemistry 43 (1), 9–14. https://doi.org/10.3103/s0361521909010030.
Sepehri, S., Soleyman, R., Varamesh, A., et al., 2018. Effect of synthetic water-soluble polymers on the properties of the heavy water-based drilling fluid at high pressure-high temperature (HPHT) conditions. J. Petrol. Sci. Eng. 166, 850–856. https://doi.org/10.1016/j.petrol.2018.03.055.
Shu, B., Ma, B., 2016. The return of drilling fluid in large diameter horizontal directional drilling boreholes. Tunn. Undergr. Space Technol. 52, 1–11. https://doi.org/10.1016/j.tust.2015.11.002.
Shumaker, J.A., McClung, A.J.W., Baur, J.W., 2012. Synthesis of high temperature polyaspartimide-urea based shape memory polymers. Polymer 53 (21), 4637–4642. https://doi.org/10.1016/j.polymer.2012.08.021.
Srungavarapu, M., Patidar, K.K., Pathak, A.K., et al., 2018. Performance studies of water-based drilling fluid for drilling through hydrate bearing sediments. Appl. Clay Sci. 152, 211–220. https://doi.org/10.1016/j.clay.2017.11.014.
Sun, M., Li, Y., Sha, S., et al., 2020. The composition and structure of n-hexane insoluble-hot benzene soluble fraction and hot benzene insoluble fraction from low temperature coal tar. Fuel 262, 116511. https://doi.org/10.1016/j.fuel.2019.116511.
Szczerski, C., Naguit, C., Markham, J., et al., 2013. Short- and long-term effects of modified humic substances on soil evolution and plant growth in gold mine tailings. Water Air Soil Pollut. 224 (3), 1471. https://doi.org/10.1007/s11270-013-1471-y.
Wang, X., Lei, Y., Chen, Z., et al., 2021. Sepiolite-zeolite powder doped with capric acid phase change microcapsules for temperature-humidity control. J. Colloid Interface Sci. 595, 25–34. https://doi.org/10.1016/j.jcis.2021.03.106.
Zhang, W., Shen, H., Wang, Y., et al., 2016. Grafting lignite with sulformethal phenoldehy resin and their performance in controlling rheological and filtration properties of water–bentonite suspensions at high temperatures. J. Petrol. Sci. Eng. 144, 84–90. https://doi.org/10.1016/j.petrol.2016.03.004.
Zhao, S., Yan, J., Shu, Y., et al., 2008. Rheological properties of oil-based drilling fluids at high temperature and high pressure. J. Cent. S. Univ. Technol. 15 (S1), 457–461. https://doi.org/10.1007/s11771-008-0399-7.